



Characterization of Polymer Tantalum Capacitors, FY11

Penelope Spence
Jet Propulsion Laboratory
Pasadena, California

Erik Reed
Kemet Corporation
Greenville, South Carolina

Jet Propulsion Laboratory
California Institute of Technology
Pasadena, California

JPL Publication 12-8 3/12



Characterization of Polymer Tantalum Capacitors, FY11

NASA Electronic Parts and Packaging (NEPP) Program
Office of Safety and Mission Assurance

Penelope Spence
Jet Propulsion Laboratory
Pasadena, California

Erik Reed
Kemet Corporation
Greenville, South Carolina

NASA WBS: 724297.40.49.11
JPL Project Number: 104593
Task Number: 40.49.01.06

Jet Propulsion Laboratory
4800 Oak Grove Drive
Pasadena, CA 91109

<http://nepp.nasa.gov>

This research was carried out at the Jet Propulsion Laboratory, California Institute of Technology, and was sponsored by the National Aeronautics and Space Administration Electronic Parts and Packaging (NEPP) Program.

Reference herein to any specific commercial product, process, or service by trade name, trademark, manufacturer, or otherwise, does not constitute or imply its endorsement by the United States Government or the Jet Propulsion Laboratory, California Institute of Technology.

Copyright 2012. All rights reserved.

TABLE OF CONTENTS

Abstract.....	1
1.0 Introduction	2
2.0 Board Mounting.....	3
3.0 Time-to-Failure Analysis	4
4.0 Acceleration Models.....	17
5.0 Summary and Conclusions	20
6.0 References.....	21

ABSTRACT

This effort is the continuation of a three-phase task to characterize tantalum polymer capacitors. Phase 1 included the history of tantalum capacitors from wet to solid, an introduction and comparison between manganese dioxide (MnO_2) and polymer tantalum capacitors, a discussion on different polymer types, and a summary of some typical electrical characteristics.

Industry has moved away from wet tantalum capacitors due to limitations of the technology. One limitation of wet tantalum technology is the electrolyte used to be able to escape from the package resulting in the capacitor slowly failing open. Current military-grade wet tantalum capacitors have robust packages that prevent leakage, unless damage is caused during handling or soldering. They also have poor performance at low temperatures since the charge carriers become less mobile. One benefit of wet tantalum technology is its self-healing capabilities. Since the anode is always in electrolyte, new oxide forms easily (an environment similar to the original dielectric formation).

Solid tantalum technology offers some improvements over wet tantalum technology. They are smaller in size and exhibit better electrical performance. Solid tantalum capacitors are also self-healing, have less capacitance roll-off, and demonstrate lower dissipation factor (DF) and equivalent series resistance (ESR) [1].

Conducting polymer material has been introduced as a candidate to replace MnO_2 . Polymers are more conductive than MnO_2 and have no ignition problems. These capacitors have even lower ESR and improved high-frequency performance, but higher leakage current. The low-temperature deposition of the polymer during manufacture causes less damage to the dielectric compared to the high-temperature conversion needed for MnO_2 . However, polymer material is less thermally stable and starts to break down around 200°C . For higher rated voltages, the breakdown and life test advantages are reduced [1].

Phase 2 presented independent competitive electrical performance data, dielectric robustness data, and reliability data. Performance advantages demonstrated by the polymer capacitors from these tests greatly suggest they should be considered for high-reliability space applications. The claims of lower ESR and better stability of capacitance versus frequency and temperature were established. Electrical performance at temperatures of -55°C was much superior to that of comparable MnO_2 technology. Tantalum polymer capacitors showed exceptional robustness against rapid charging above rated voltage, while some tantalum MnO_2 capacitors demonstrated higher breakdown voltages. Performance during the 85°C rated voltage life test of polymer versus MnO_2 technology was comparable, but tantalum polymer technology has not matured to the point of being routinely used in harsh operating conditions such as 125°C or high humidity situations [2].

Phase 3 is intended to conduct highly accelerated time-to-failure testing and develop acceleration models to predict performance at rated conditions. Tantalum polymer devices of several different voltage ratings will be tested and assessed. At this time, only data associated with devices rated at 4 V are presented.

1.0 INTRODUCTION

The focus of this project is to assess the lifetime of polymer tantalum capacitors at maximum rated conditions, noting distributions of failures in time, and to study the applicability of the Weibull grading method to tantalum polymer capacitors. Devices were tested at several temperatures and voltages chosen specifically to reach wear-out in a reasonable amount of time.

The main goal is to develop an accurate acceleration model by focusing on accelerated life tests using elevated voltage and temperature conditions. A secondary goal is to compare two different manufacturers, Manufacturer A and Manufacturer B, to determine if the acceleration models developed are similar. Each part type was subjected to various test voltages at three different temperatures. The temperatures 85°C, 105°C, and 125°C were chosen for the experiment. Time-to-failure data were collected on a computer monitoring system. Failures were defined as devices that had blown a 1A fuse. Applied test voltages for each temperature varied and were determined by scouting tests. The goal of scouting was to achieve sufficient voltage acceleration that all of the parts would fail in a reasonable amount of time (less than roughly 1,000 hours).

Table 1-1 summarizes the capacitors chosen for evaluation. At this time, complete data are only available for the 220 μF , 4 V devices.

Testing was modeled after that described in [3]. Tantalum polymer capacitor failures-in-time should produce a lognormal time-to-failure distribution with a very steep slope indicating wear-out, instead of a shallow slope time-to-failure distribution as is typically produced by MnO_2 type capacitors.

Figure 1-1 shows an example of time-to-failure data for B-case, 100 μF , 6 V devices taken from Figure 6 in [3]. It depicts data taken at a temperature of 105°C at several different voltage accelerations. It was expected that the D-case 4 V, 6 V, 10 V, and 16 V devices chosen for this experiment would behave in a similar fashion. What was observed was not always what was expected.

Table 1-1. Tantalum Polymer Capacitors

Capacitance (μF)	Rated Voltage (V)
220	4
330	6
100	10
47	16

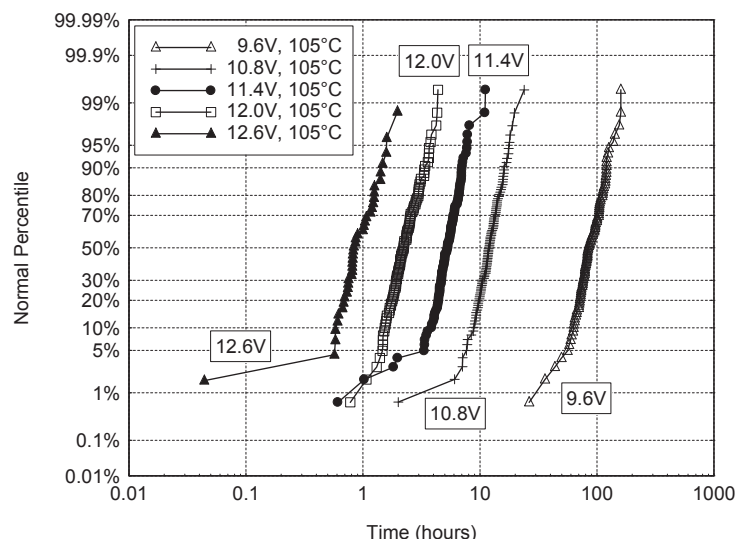


Figure 1-1. Tantalum Polymer Lognormal Distribution Example [3]

2.0 BOARD MOUNTING

The capacitors to be tested were mounted to test cards using standard convection reflow since this is the most often used process in industry. Figure 2-1 and Table 2-1 show an example of the convection reflow temperature profile used to solder the capacitors to the test boards.

The blue line in Figure 2-1 is the temperature measured by a thermocouple soldered to a PCB board that passed through the convection reflow oven. Table 2-2 shows the temperatures for each zone of the reflow oven. The reflow oven was a Heller 1500SX with KIC profile software.

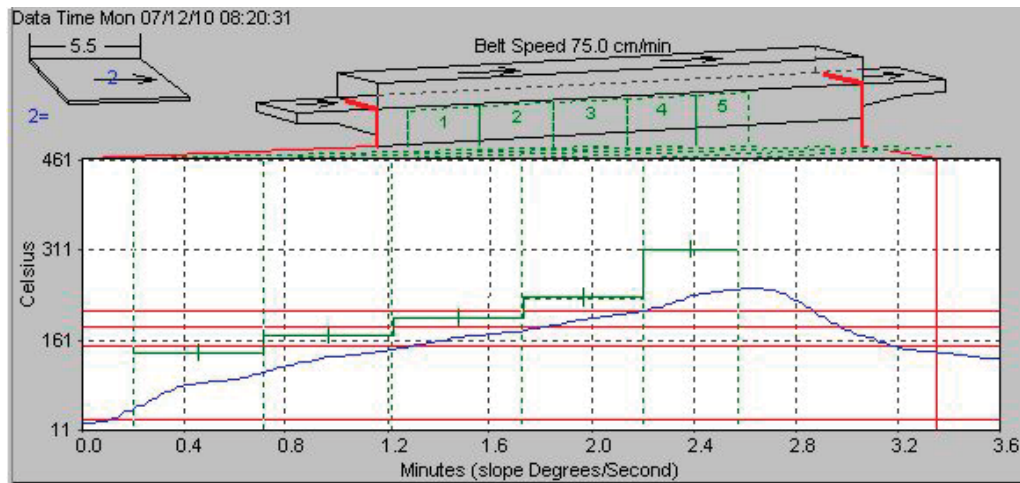


Figure 2-1. Typical Convection Solder Reflow Temperature Profile

Table 2-1. Convection Solder Reflow Temperature Profile Details

	Peak	Max Rising Slope	Rising Time Above 30	Rising Time Between 30/150	Total Time Above 150	Total Time Between 150/183	Total Time Above 183	Total Time Between 183/210	Total Time Above 210
2	245.0	4.26	151.06	70.40	115.07	44.43	70.64	29.53	41.11
TC Mean	245.0	4.26	151.06	70.40	115.07	44.43	70.64	29.53	41.11
TC SD	—	—	—	—	—	—	—	—	—
TC Range	0.0	0.00	0.00	0.00	0.00	0.00	0.00	0.00	0.00

Table 2-2. Convection Reflow Oven Settings

Zone	1	2	3	4	5
Temperature (°C)	140	170	200	230	315

3.0 TIME-TO-FAILURE ANALYSIS

The 100 μ F, 10 V polymer capacitors were the first to undergo accelerated life testing.

Figures 3-1 and 3-2 show data collected at a temperature of 85°C and a test voltage of 18 V for both manufacturers. The data do not follow the expected trend (based on Figure 1-1) and appear more like Weibull plots of MnO₂-cathode tantalum capacitor failures. Due to this unexpected behavior, testing for Manufacturer A was halted around 100 hours and Manufacturer B just shy of 9,000 hours.

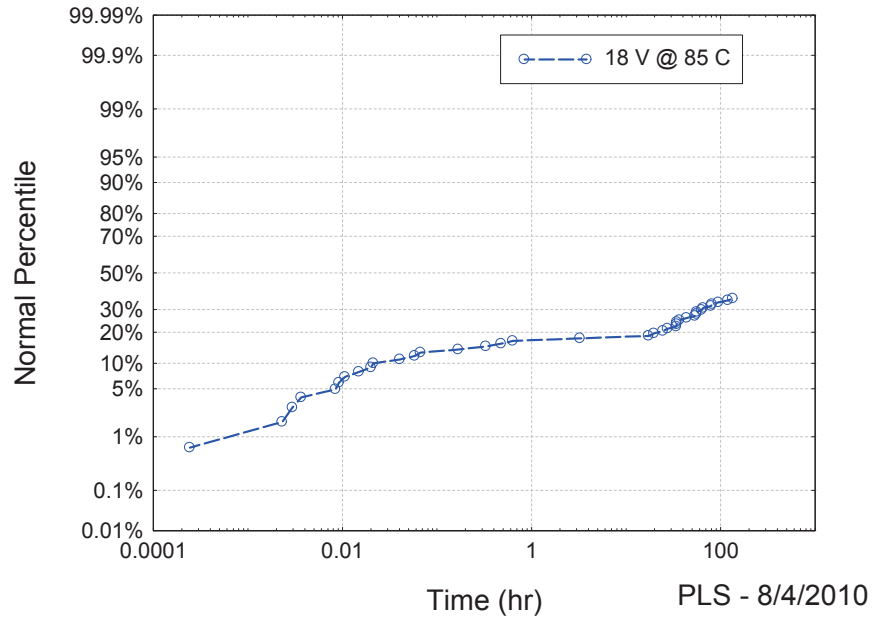


Figure 3-1. Manufacturer A, 100 μ F, 10 V Tested at 85°C

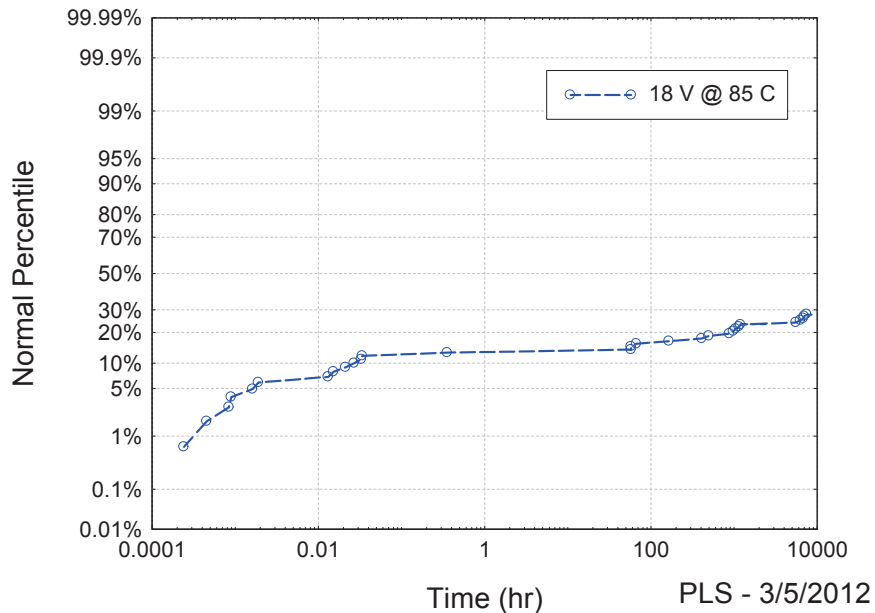


Figure 3-2. Manufacturer B, 100 μ F, 10 V Tested at 85°C

Similar behavior is seen in the higher voltage tantalum polymer parts, rated 25 V and above [4]. Figure 3-3 identifies various distinct patterns in 35 V tantalum polymer time-to-failure distributions that can be identified in Figure 3-4 for the 10 V parts of Figure 3-2. In Figure 3-4, the regions have been identified in a manner similar to that employed in Figure 3-3. The first region consists of initial failures at the beginning of the test that increase with increasing test voltage. The second flat region consists of failures occurring slowly over time. Time in this period seems to increase with decreasing test voltage. The third and fourth regions, which are clearly separated in Figure 3-3, seem to be comingled in Figure 3-4. The third region is the area of interest considered to be wear-out. Here, many failures are expected to occur in a relatively short period of time [4].

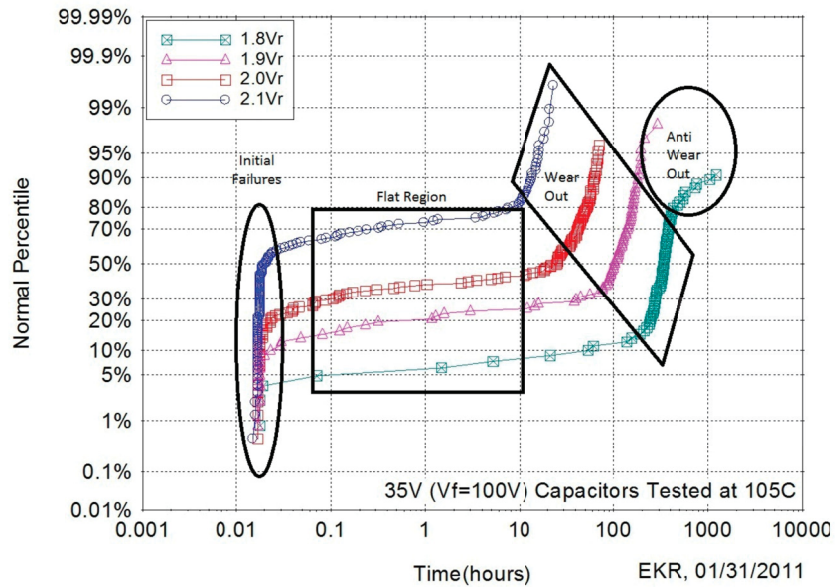


Figure 3-3. Lognormal Plot of Failure Percentile versus Time-to-Failure at Various Accelerated Voltages for Tests Performed at 105°C. 15µF, 35 V Experimental Polymer Capacitors [4]

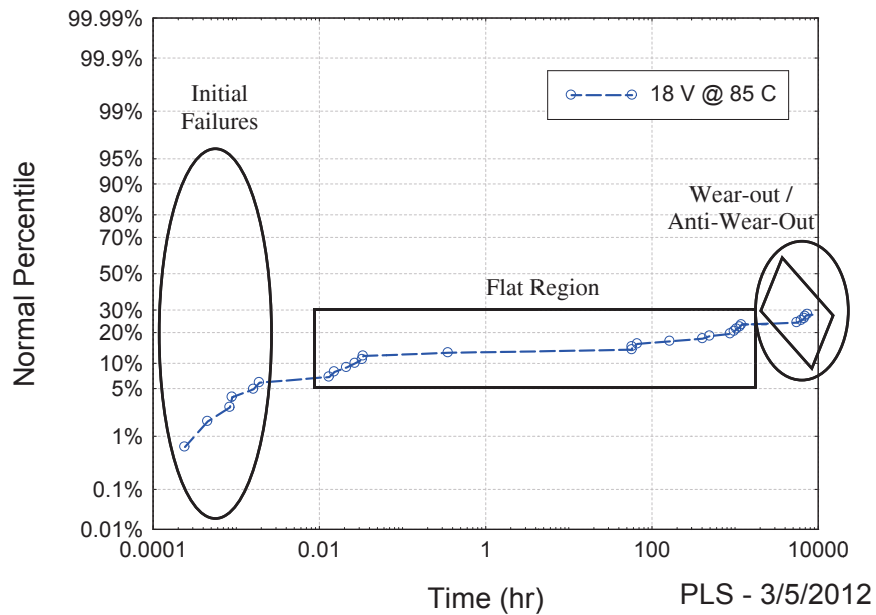


Figure 3-4. Manufacturer B, 100 µF, 10 V Tested at 85°C, Different Failure Regions

The final region, anti-wear-out, is not yet well understood; however, it is believed that de-doping of the polymer material is occurring. As the polymer next to the dielectric becomes non-conductive, the capacitance decreases and the ESR increases. Evidence of this can be seen in the pre- and post-time-to-failure capacitance and ESR lognormal distributions shown in Figures 3-5 and 3-6. Many of the surviving capacitors exhibit lower capacitance values coupled with higher ESR, as is seen in the median capacitance of 101.5 μF dropping to 95.7 μF and the median ESR rising from 36.4 mOhm to 43.5 mOhm. Other capacitors remain within normal limits and continue to be candidates for wear-out.

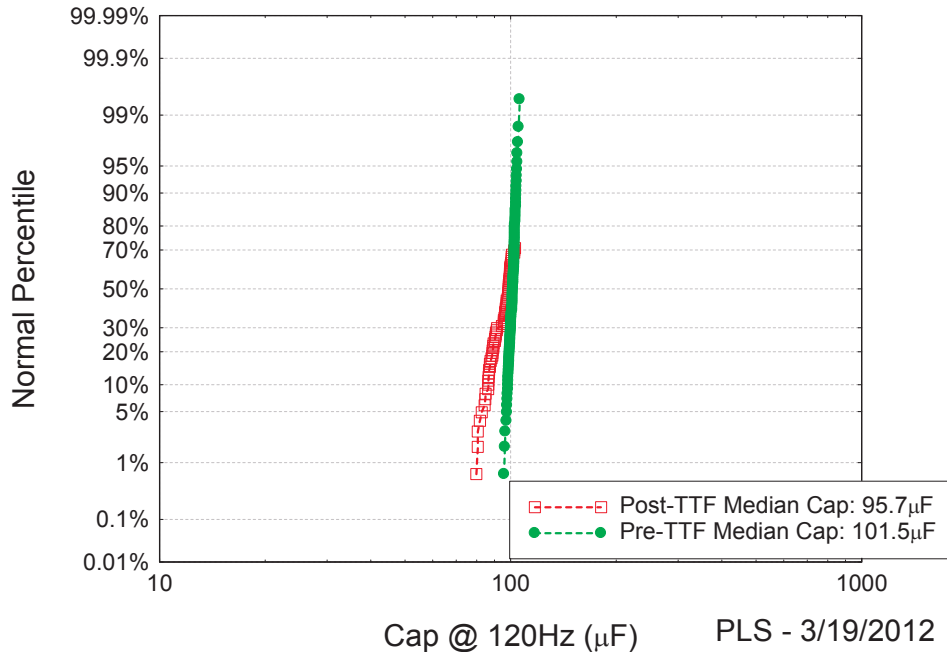


Figure 3-5. Manufacturer B, 100 μF , 10 V Tested at 85°C, 18 V, Pre- and Post-TTF Capacitance

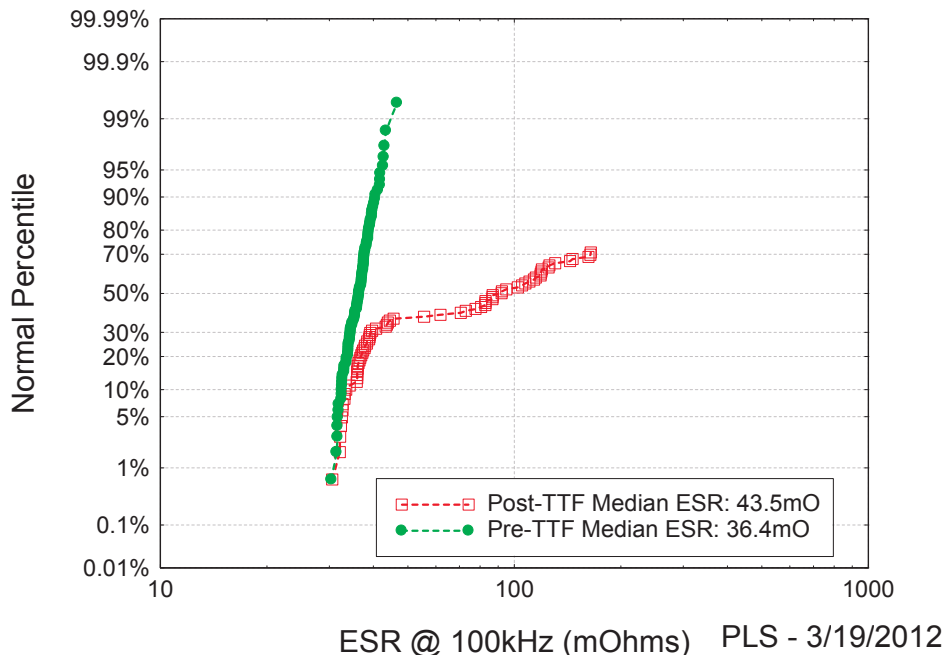


Figure 3-6. Manufacturer B, 100 μF , 10 V Tested at 85°C, 18 V, Pre- and Post-TTF ESR

Due to time constraints, testing of the 100 μF , 10 V parts was stopped and testing of the 220 μF , 4 V parts commenced. At this time, only data for the 220 μF , 4 V capacitors are available for full analysis.

Table 3-1 shows the chosen test voltages for each temperature and the resulting t_{50} times. The test voltages were chosen from scouting tests with the goal of having the highest test voltage produce t_{50} around 2 hours, the middle test voltage produce t_{50} around 10 hours, and the lowest test voltage produce t_{50} around 100 hours. A fourth test voltage (10 V) was added for Manufacturer B at a test temperature of 85°C, because it was discovered after the start of the test that the original test voltages chosen might have been too severe, introducing a new failure mechanism. The resulting t_{50} values were estimated from the time-to-failure data by using a best fit line for each of the time-to-failure distributions.

The 220 μF , 4 V capacitors made by Manufacturer A and tested at 85°C, behaved as expected as shown in Figure 3-7. Each test voltage resulted in a plot relatively parallel to the others at the fixed temperature.

The time-to-failure data for Manufacturer B in Figure 3-8 are somewhat expected and somewhat not expected. The curves in Figure 3-8 almost follow the same trend as seen in Figure 3-7, but appear to have additional sub-distributions. This is similar to the complexity of the time-to-failure distributions introduced in Figure 3-3 and highlighted for the 10 V parts in Figure 3-4. However, it appears that there may be even more complexity in the 12.4 V data of Figure 3-8.

Careful examination of Figure 3-8 reveals the expected initial failures region and flat region. However, a region of overlap is then observed between the flat and wear-out regions, followed by a pure wear-out region, and briefly by anti-wear-out. The anti-wear-out is followed by additional failures that are believed to be wear-out of the de-doped polymer. This results in short-circuit failure of the capacitors, which then blow their 1 A fuse. Evidence of anti-wear-out de-doping of the conductive polymer appears in the subsequent discussion where capacitance loss and ESR increases demonstrate loss of conduction in the conductive polymer cathode.

Table 3-1. Testing Conditions and Resulting t_{50} Values

Manufacturer A: 220 μF, 4 V					
85°C		105°C		125°C	
V_{Test} (V)	t_{50} (hr)	V_{Test} (V)	t_{50} (hr)	V_{Test} (V)	t_{50} (hr)
10	169	8.8	105	8.8	13
10.8	46	9.6	33	9.2	8.6
11.6	18	10.4	11	9.6	4.5
Manufacturer B: 220 μF, 4 V					
85°C		105°C		125°C	
V_{Test} (V)	t_{50} (hr)	V_{Test} (V)	t_{50} (hr)	V_{Test} (V)	t_{50} (hr)
10	2,000	10	110	8.8	50
10.8	300	10.8	26	9.2	28
11.6	13	11.6	10	9.6	19
12.4	0.4	-	-	-	-

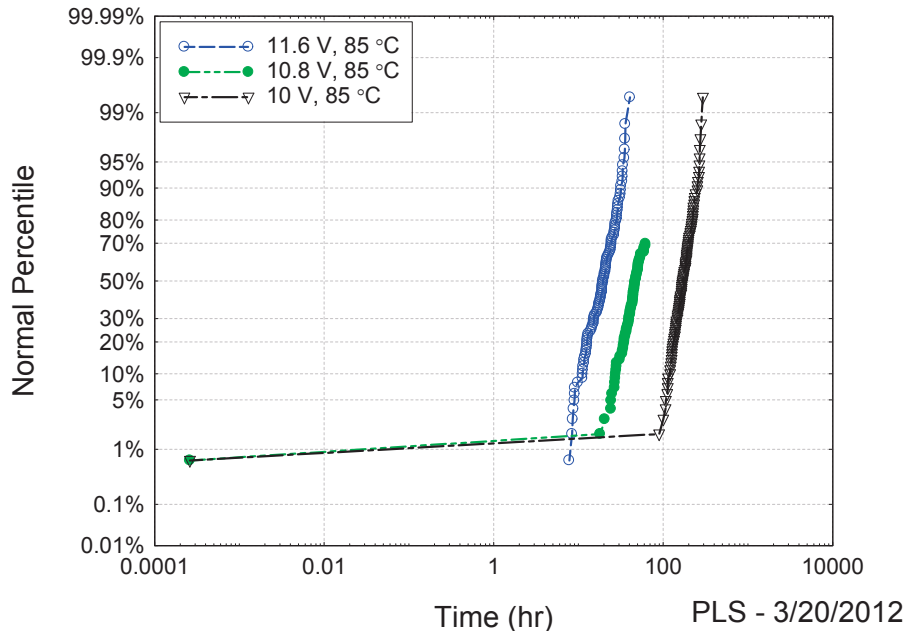


Figure 3-7. Manufacturer A, 220 μ F, 4 V tested at 85°C

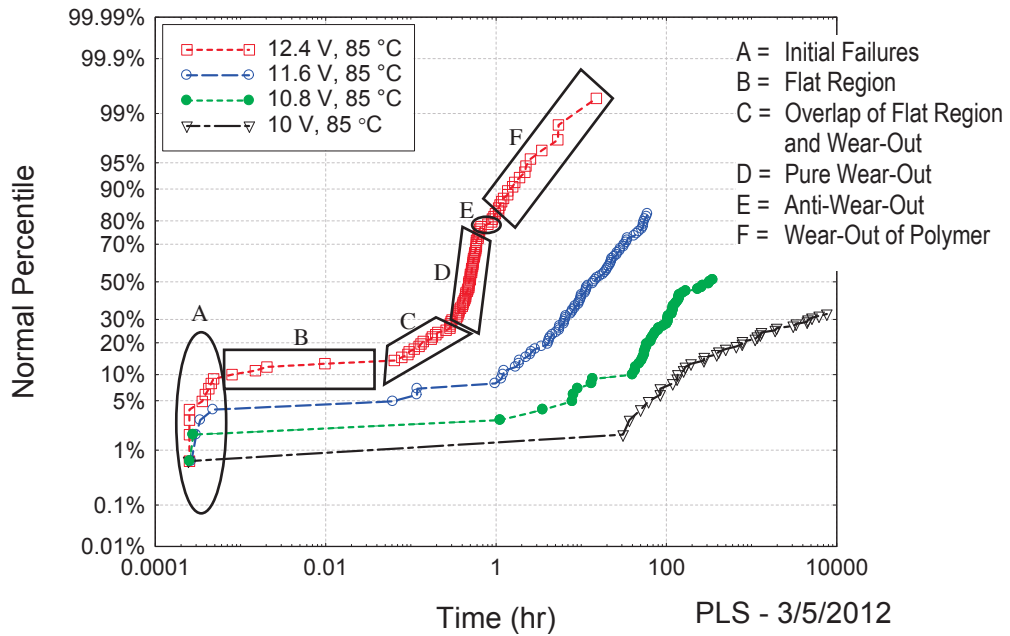


Figure 3-8. Manufacturer B, 220 μ F, 4 V Tested at 85°C

An analysis of the capacitance and ESR values before and after time-to-failure testing clearly shows that anti-wear-out is present. For Manufacturer B parts tested at 10 V, all surviving capacitors have decreased capacitance values in Figure 3-9 and increased ESR in Figure 3-10. The shallow slope of the final time-to-failure data in Figure 3-8 hints at this phenomenon where the rate of blown-out 1 A fuses slows as the normally conductive polymer becomes less conductive.

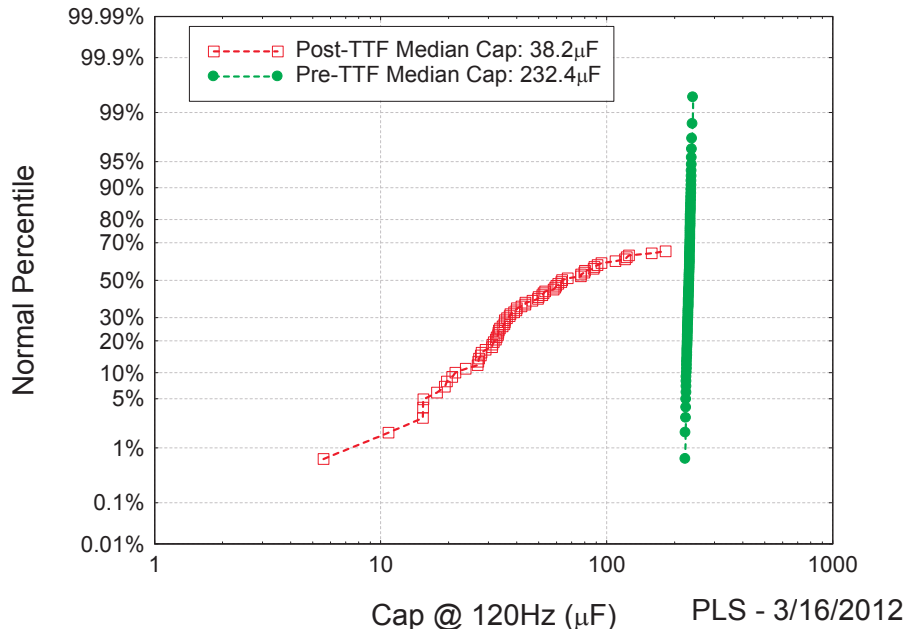


Figure 3-9. Manufacturer B, 220 μF , 4 V Tested at 85°C, 10 V, Pre- and Post-TTF Capacitance

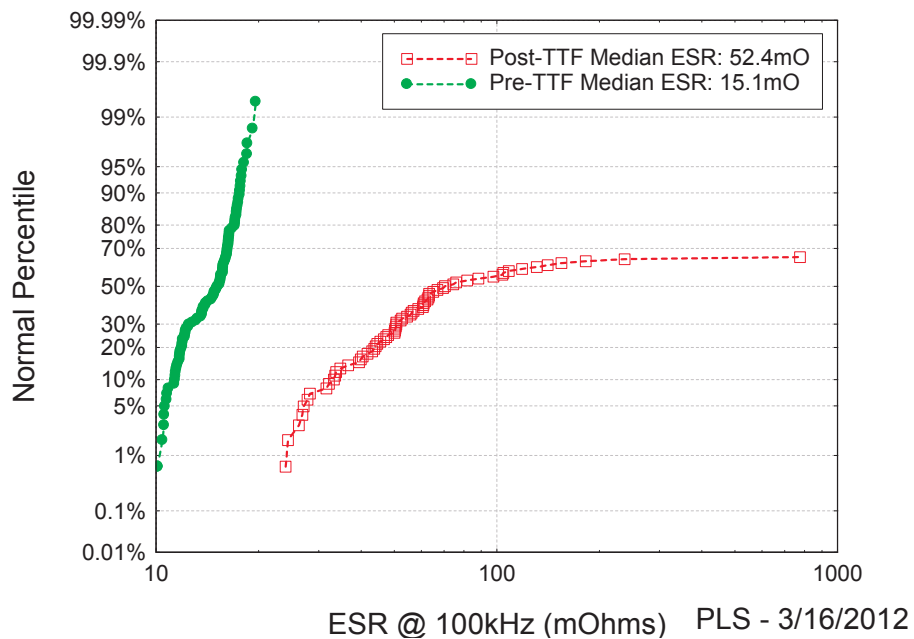


Figure 3-10. Manufacturer B, 220 μF , 4 V Tested at 85°C, 10 V, Pre- and Post-TTF ESR

The remaining capacitors from the 10.8 V distribution in Figure 3-8 are in the anti-wear-out stage with decreased capacitance in Figure 3-11 coupled with increased ESR in Figure 3-12.

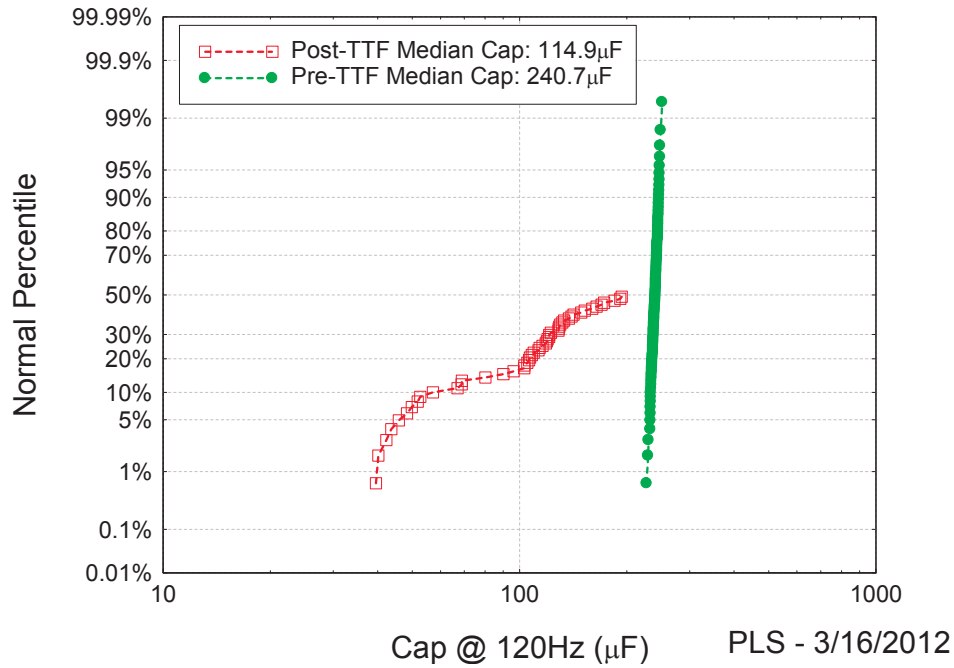


Figure 3-11. Manufacturer B, 220 µF, 4 V Tested at 85°C, 10.8 V, Pre- and Post-TTF Capacitance

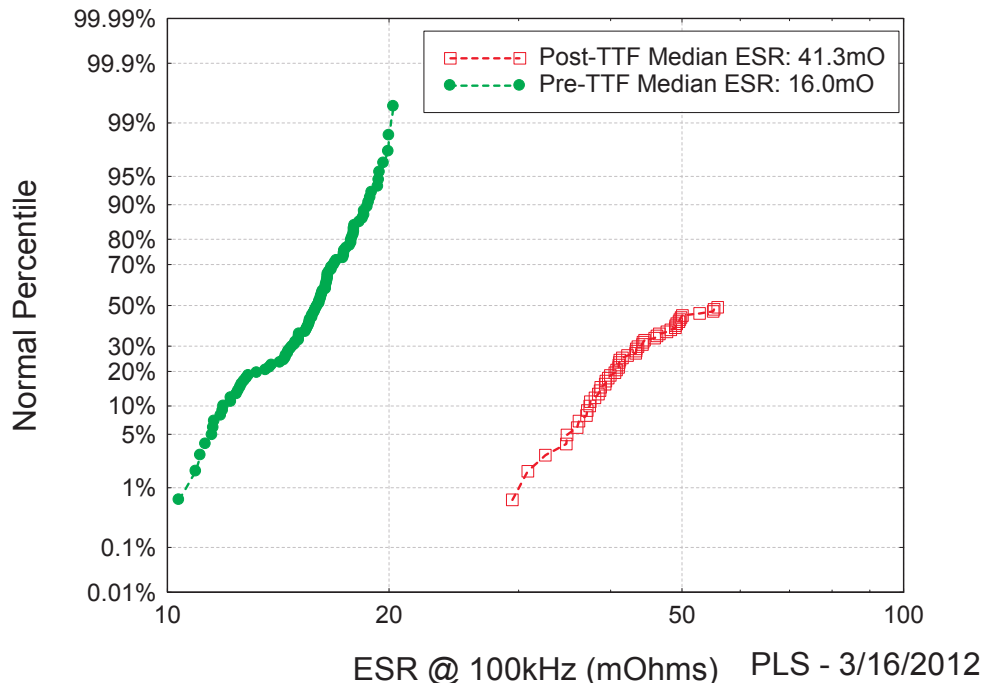


Figure 3-12. Manufacturer B, 220 µF, 4 V Tested at 85°C, 10.8 V, Pre- and Post-TTF ESR

Data for Manufacturer A in Figure 3-13 at 105°C seem to exhibit a more uniform relationship among the failure distributions generated at the different test voltages.

Figure 3-14 demonstrates more pronounced evidence of the multiple distributions within each 100-piece test sample for the times to failure of Manufacturer B at the test voltage 11.6 V. Generally, the times to failure decrease as the test voltage rises, as expected, but the shape of the distribution also changes with increasing voltage, suggesting introduction of a new degradation mechanism.

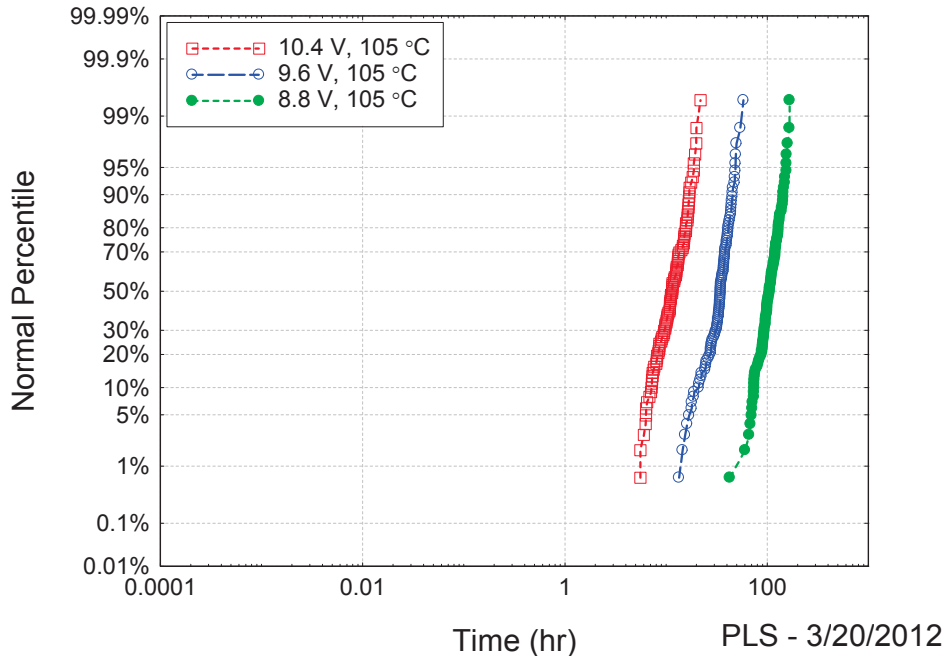


Figure 3-13. Manufacturer A, 220 μ F, 4 V Tested at 105°C

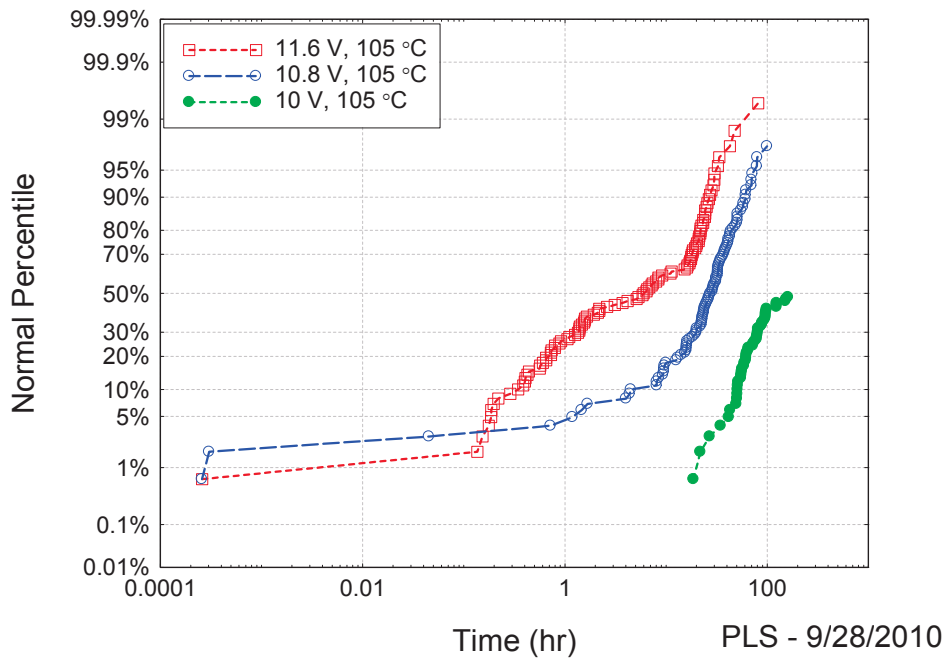


Figure 3-14. Manufacturer B, 220 μ F, 4 V Tested at 105°C

Figures 3-15 and 3-16 reveal the same decreased capacitance and increased ESR. Looking at the time-to-failure distribution curve in Figure 3-14 of the parts tested at 10 V, the failure distribution curve exhibits the vertical area associated with wear-out followed by the shallower slope of anti-wear-out where the failures start occurring less frequently.

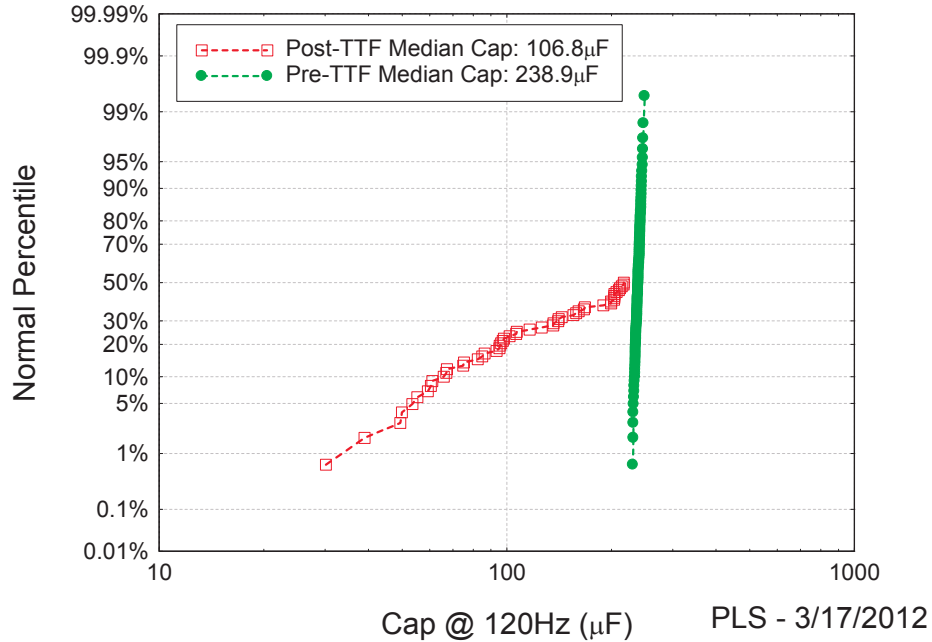


Figure 3-15. Manufacturer B, 220 μF , 4 V Tested at 105°C, 10 V, Pre- and Post-TTF Capacitance

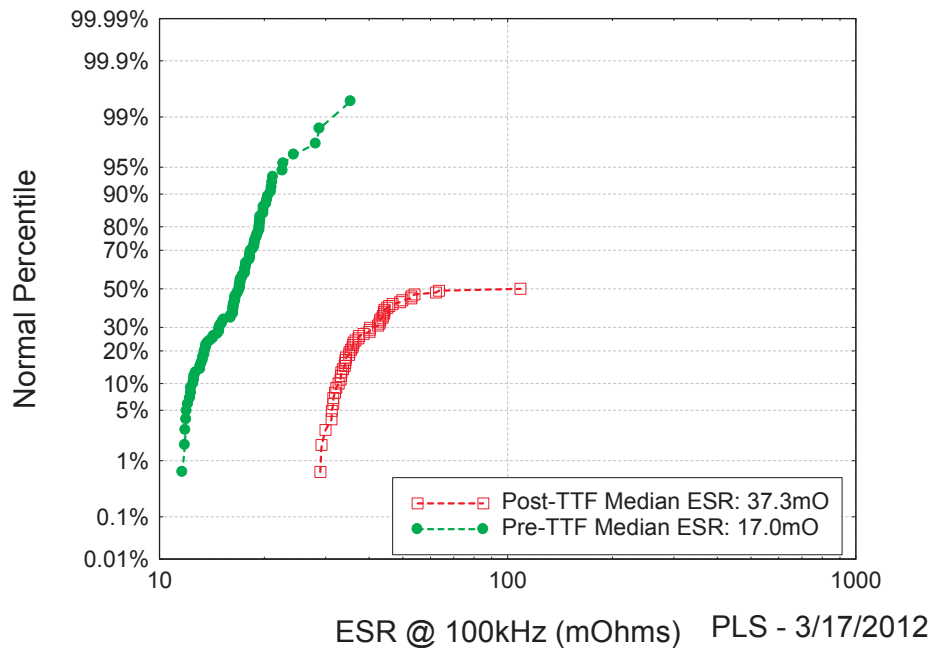


Figure 3-16. Manufacturer B, 220 μF , 4 V Tested at 105°C, 10 V, Pre- and Post-TTF ESR

The last two surviving capacitors tested at 105°C and 10.8 V have decreased capacitance in Figure 3-17 and increased ESR in Figure 3-18. The distribution curve in Figure 3-14 has a very slight curve at the end suggesting that the parts have entered anti-wear-out.

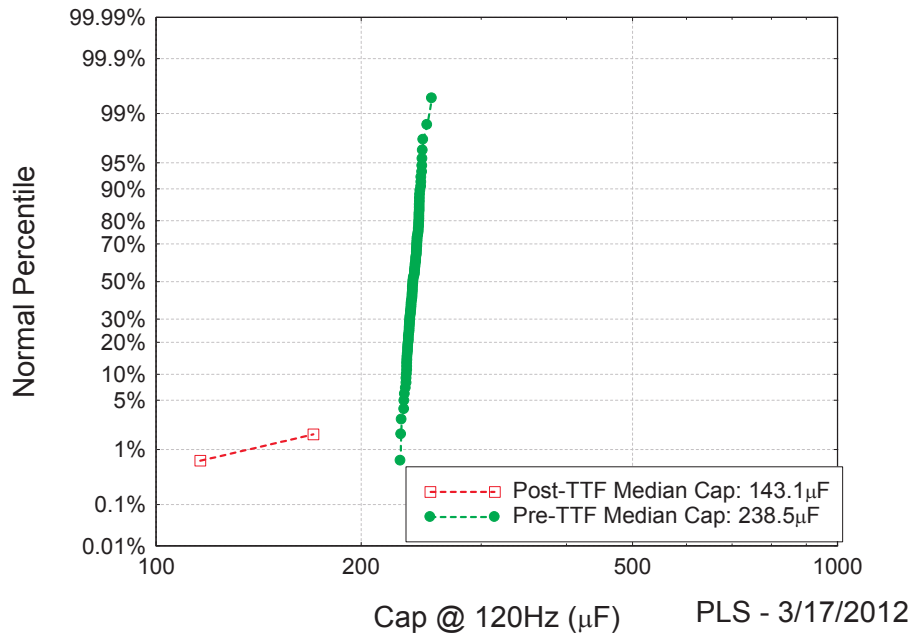


Figure 3-17. Manufacturer B, 220 µF, 4 V Tested at 105°C, 10.8 V, Pre- and Post-TTF Capacitance

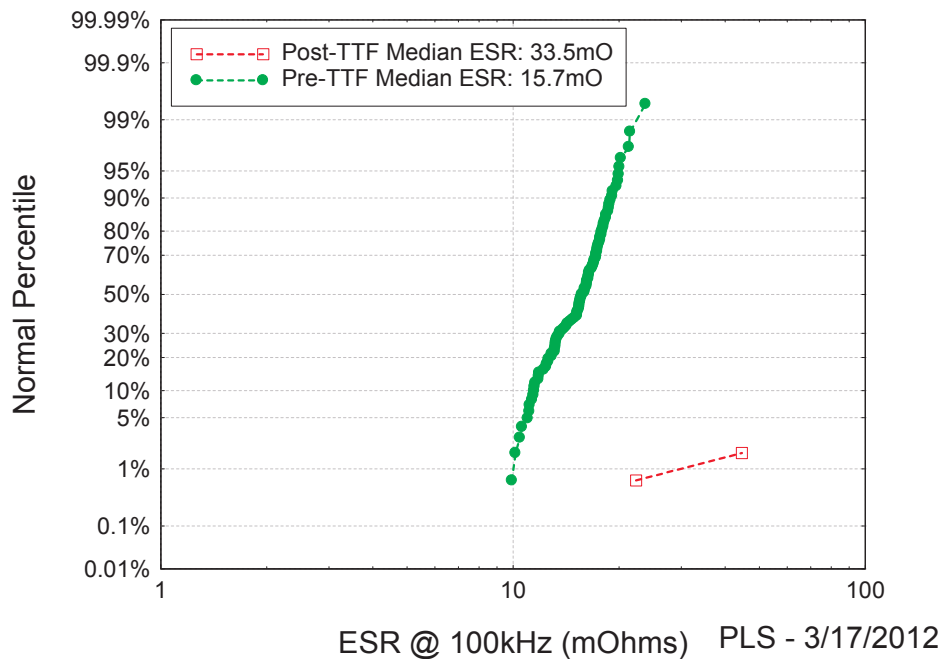


Figure 3-18. Manufacturer B, 220 µF, 4 V Tested at 105°C, 10.8 V, Pre- and Post-TTF ESR

Figure 3-19 at 125°C for Manufacturer A shows similar results to Figures 3-7 and 3-13. These parts continue to behave as expected with no evidence of anti-wear-out behavior.

The data of Figure 3-20 for Manufacturer B have shallower slopes than those seen in the plots for Manufacturer A hinting that anti-wear-out is active. The curves do not contain the bimodal distributions seen in Figures 3-8 and 3-14.

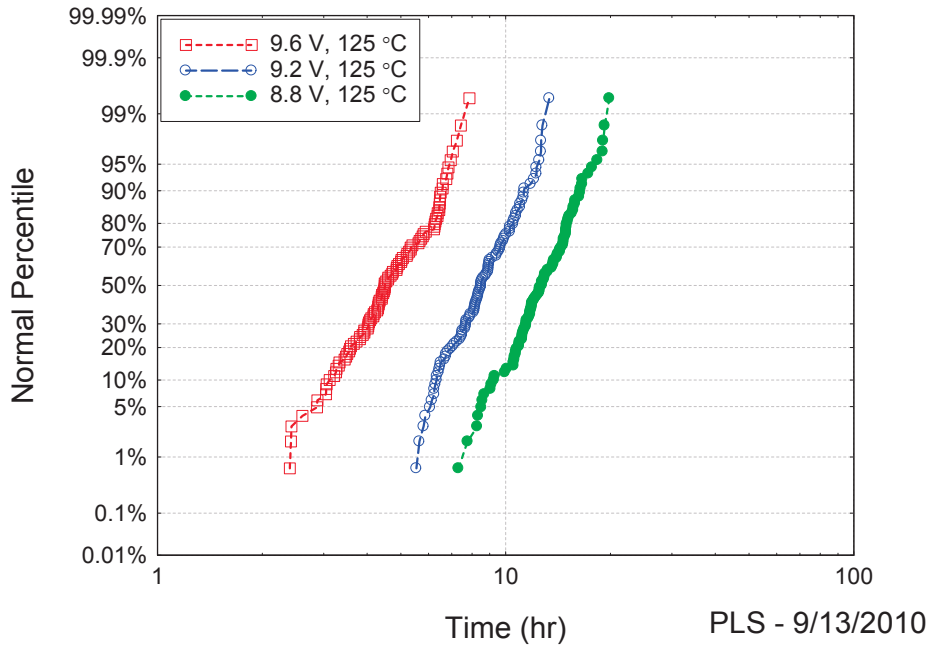


Figure 3-19. Manufacturer A, 220 μ F, 4 V Tested at 125°C

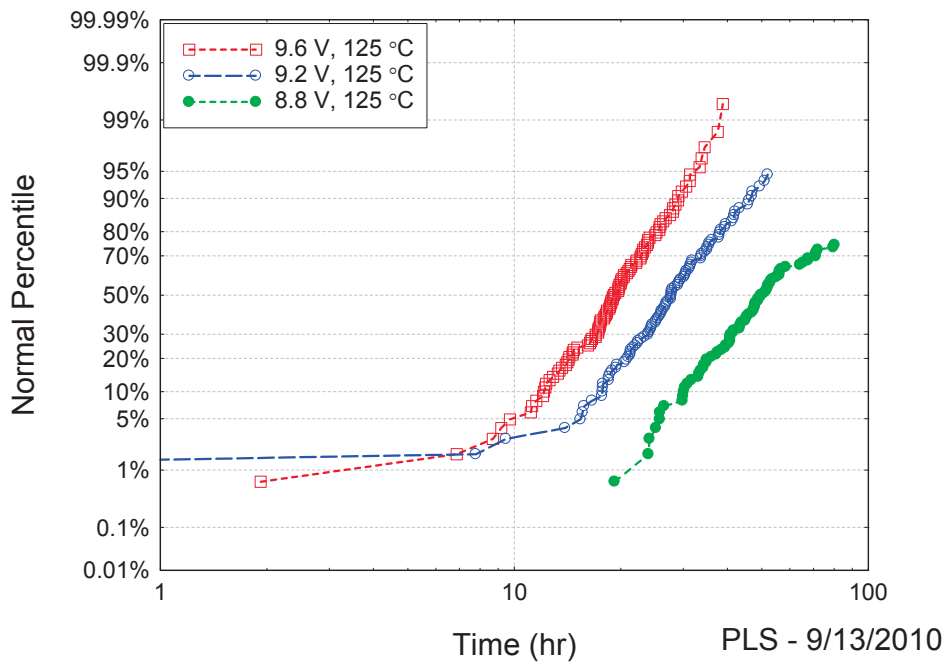


Figure 3-20. Manufacturer B, 220 μ F, 4 V Tested at 125°C

The decreased slope at the end of the distribution in Figure 3-20 for parts tested at 8.8 V suggests that parts have entered anti-wear-out. The surviving parts were tested and all were found to have decreased capacitance in Figure 3-21 and increased ESR in Figure 3-22 indicative of polymer de-doping.

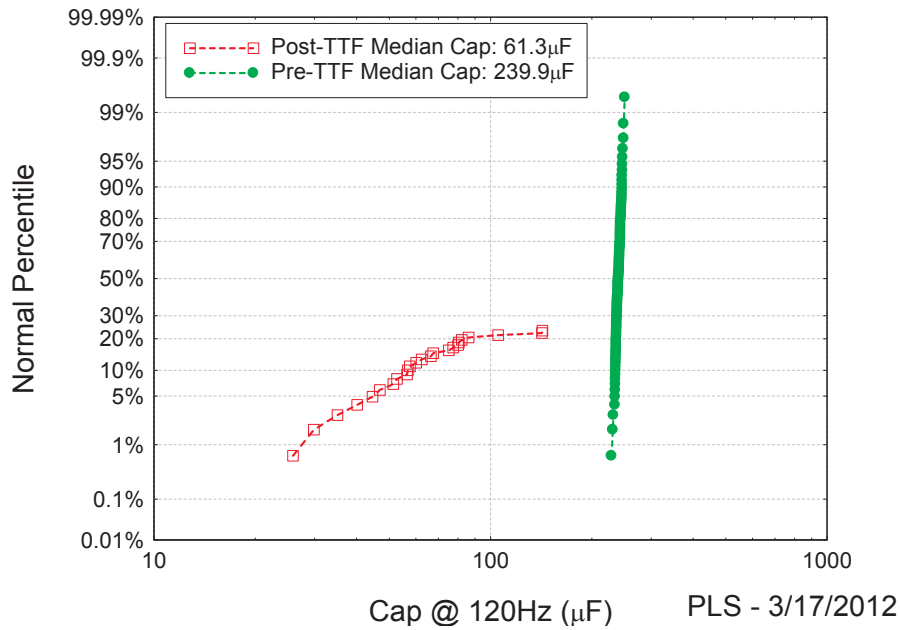


Figure 3-21. Manufacturer B, 220 µF, 4 V Tested at 125°C, 8.8 V, Pre- and Post-TTF Capacitance

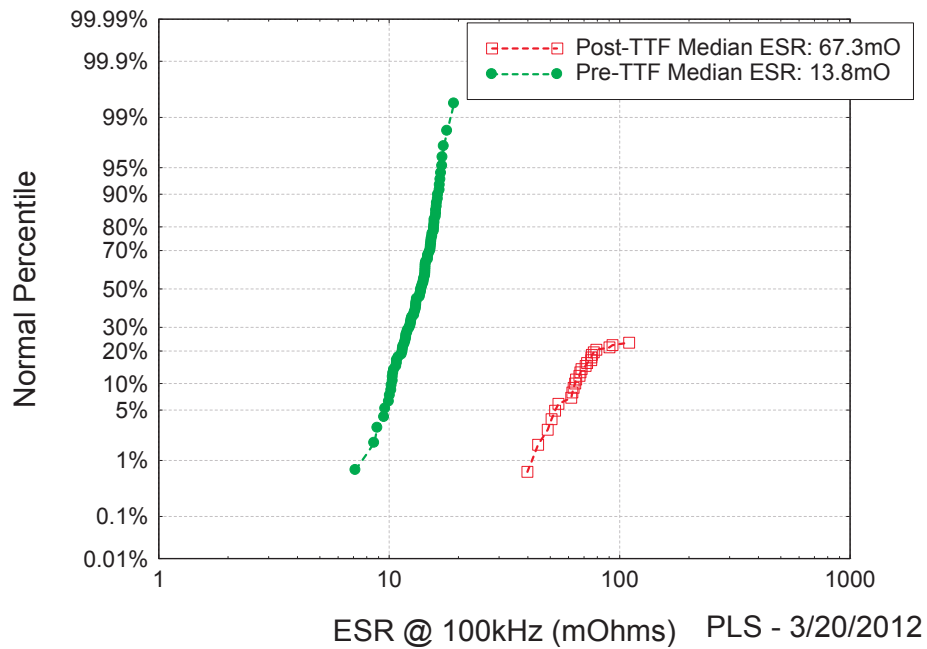


Figure 3-22. Manufacturer B, 220 µF, 4 V Tested at 125°C, 8.8 V, Pre- and Post-TTF ESR

The capacitance and ESR data of Figures 3-23 and 3-24 for the 9.2 V distribution curve in Figure 3-20 show the same anti-wear-out trend seen in Figure 3-21 and Figure 3-22. This suggests that the apparent increased life in Figure 3-20 is the result of polymer de-doping and loss of polymer conductivity rather than any inherent improvement in dielectric robustness. The shallower slope of all the time-to-failure curves in Figure 3-20 supports this observation.

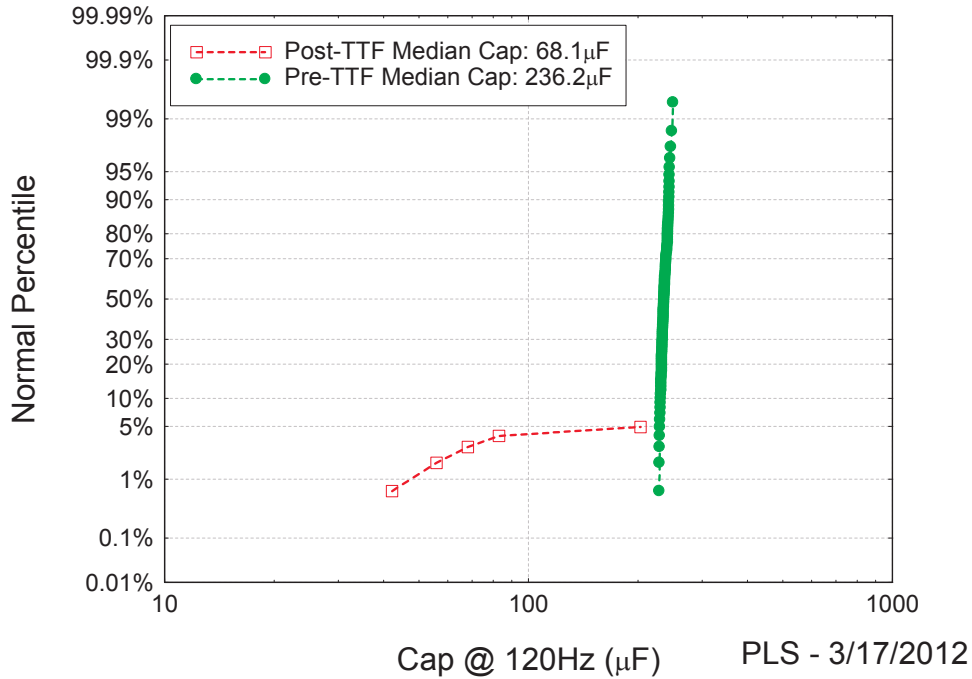


Figure 3-23. Manufacturer B, 220 μF, 4 V Tested at 125°C, 9.2 V, Pre- and Post-TTF Capacitance

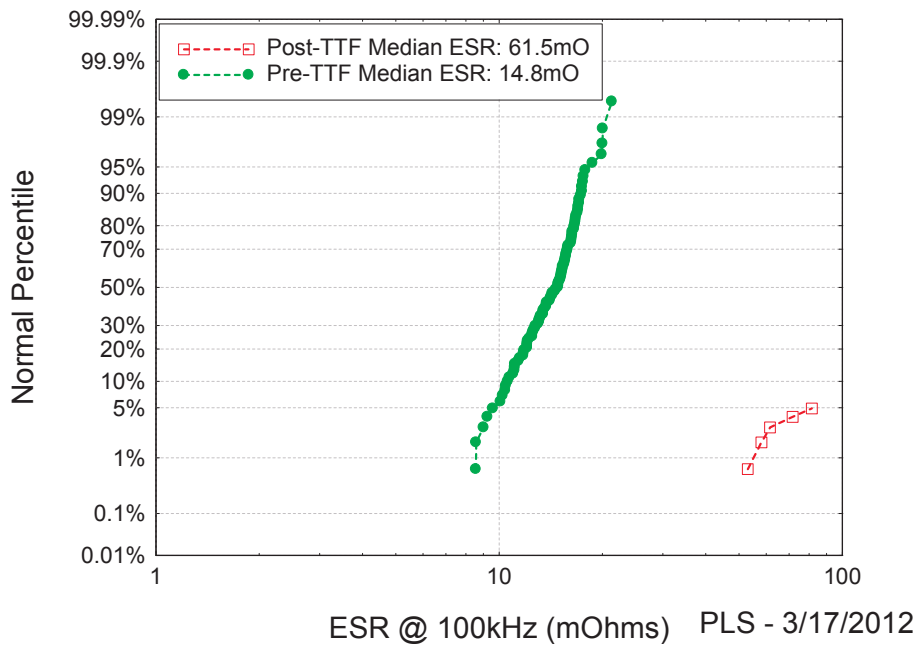


Figure 3-24. Manufacturer B, 220 μF, 4 V Tested at 125°C, 9.2 V, Pre- and Post-TTF ESR

4.0 ACCELERATION MODELS

The equation proposed by Prokopowicz and Vaskas shown in Equation (1) was chosen for the acceleration model [3].

$$A = \frac{t_1}{t_2} = \left(\frac{V_2}{V_1} \right)^\eta e^{\left[\frac{E_a}{k} \left(\frac{1}{T_1} - \frac{1}{T_2} \right) \right]} \quad (1)$$

The formula can be broken down into two parts to calculate voltage acceleration and temperature acceleration separately. The voltage stress exponent (η) and activation energy (E_a) must be derived experimentally from time-to-failure data. Median life values (t_{50}) from the failure distributions are used for t_1 and t_2 . The constant k is Boltzmann's constant, $8.62 \cdot 10^{-5}$ eV/K [3].

The t_{50} times at the various temperatures and test voltages are plotted on a log-log scale in Figure 4-1 to linearize the power law form of voltage acceleration in Equation (1). This facilitates estimation of η , which is the voltage ratio exponent that predicts failure acceleration due to increasing test voltage.

The data in the voltage acceleration plot for Manufacturer A shown in Figure 4-1 are pretty well behaved. It is possible to project back to rated voltage fairly easily. The slopes of the lines generated by the t_{50} data points are similar and have a decreasing voltage ratio exponent (η) as the temperature rises. This response is consistent with the results published in [3].

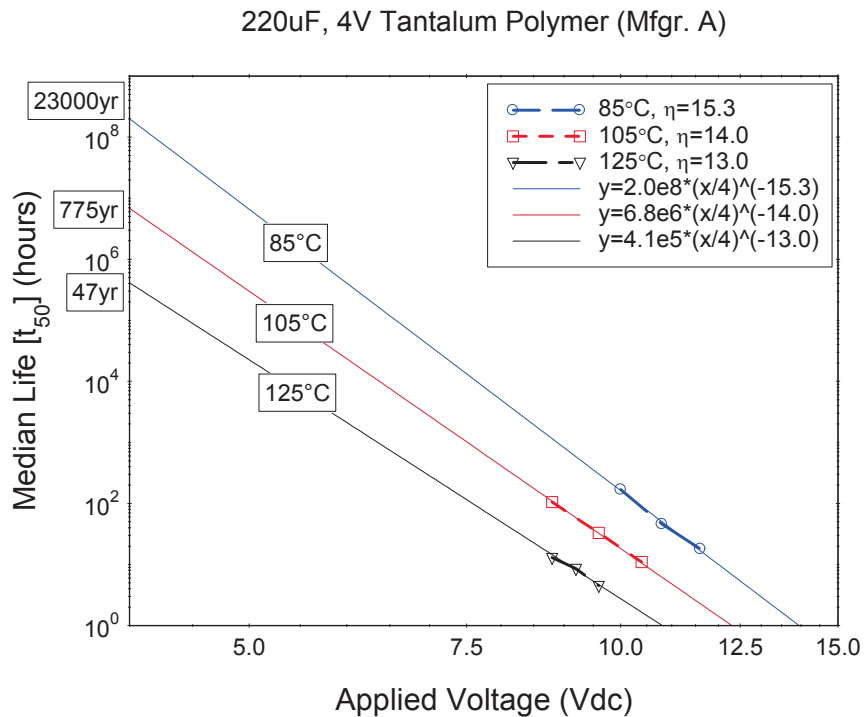


Figure 4-1. Manufacturer A Voltage Acceleration

In contrast, the data for Manufacturer B in Figure 4-2 are not as ideal. The 125°C data appear fine at η of 10.3, but the slope for the 105°C data begins to get very steep at η of 16.3 and the data are questionable. The data for 85°C certainly do not support a meaningful extrapolation to lower test voltages. This means that in the effort to minimize test time, the test voltages were selected to be too high. The test voltages were too close to the oxide formation voltage and excite a new failure mechanism, which has a much higher voltage ratio exponent than the wear-out mechanism that is dominant at or below rated voltage. The time-to-failure slopes are increasing as 12.4 V is approached. If 12.4 V were used at the temperatures of 105°C and 125°C, it is likely the same results would be observed. This is evidence that there are absolute limits to how much this testing can be accelerated.

Manufacturer A's t_{50} times are plotted versus inverse absolute temperature ($1/T$, with T in Kelvin) in Figure 4-3. This linearizes the Arrhenius expression for temperature acceleration, allowing straight lines to be fit to the curves in order to estimate activation energy in electron volts (eV) at various test voltages. Unfortunately, the same voltages at two different temperatures were only used two times (8.8 V and 9.6 V at 105°C and 125°C). A least squares line was fit to those points and the activation energy was found to be 1.35 eV at 8.8 V and 1.29 eV at 9.6 V. The higher activation energy at the lower voltage is consistent with results seen in [3].

Fit lines could not be added to the other t_{50} data points because for these groups no two tests were done at the same voltage and two temperatures. However, dashed lines with the same slope as the 9.6 V line show that the spacing between the lines is very consistent with the spacing of the test voltages. This is also consistent with the analogous temperature acceleration graph in [3].

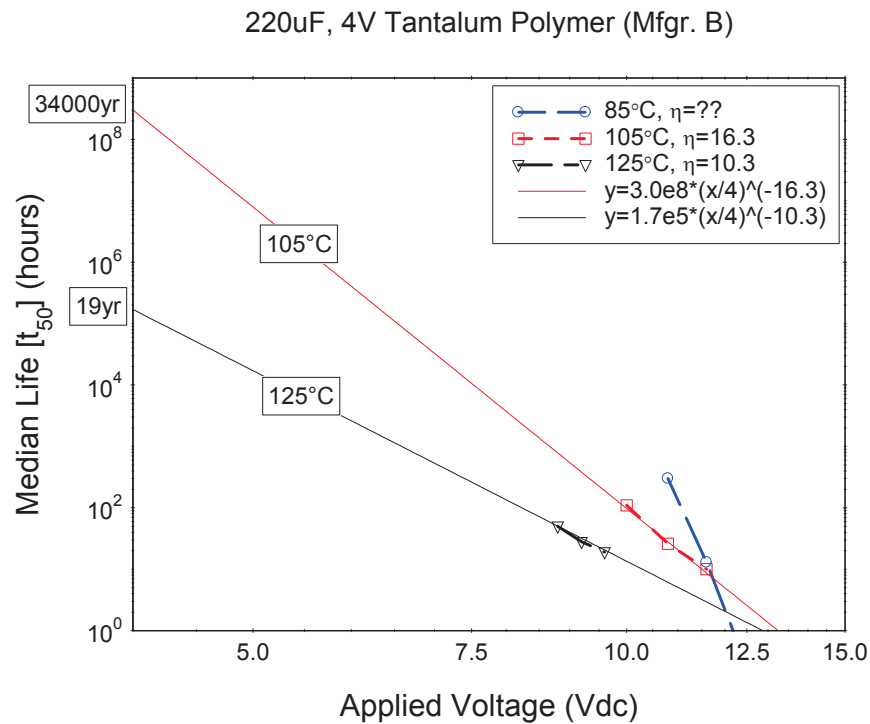


Figure 4-2. Manufacturer B Voltage Acceleration

220uF, 4V Tantalum Polymer (Mfgr. A)

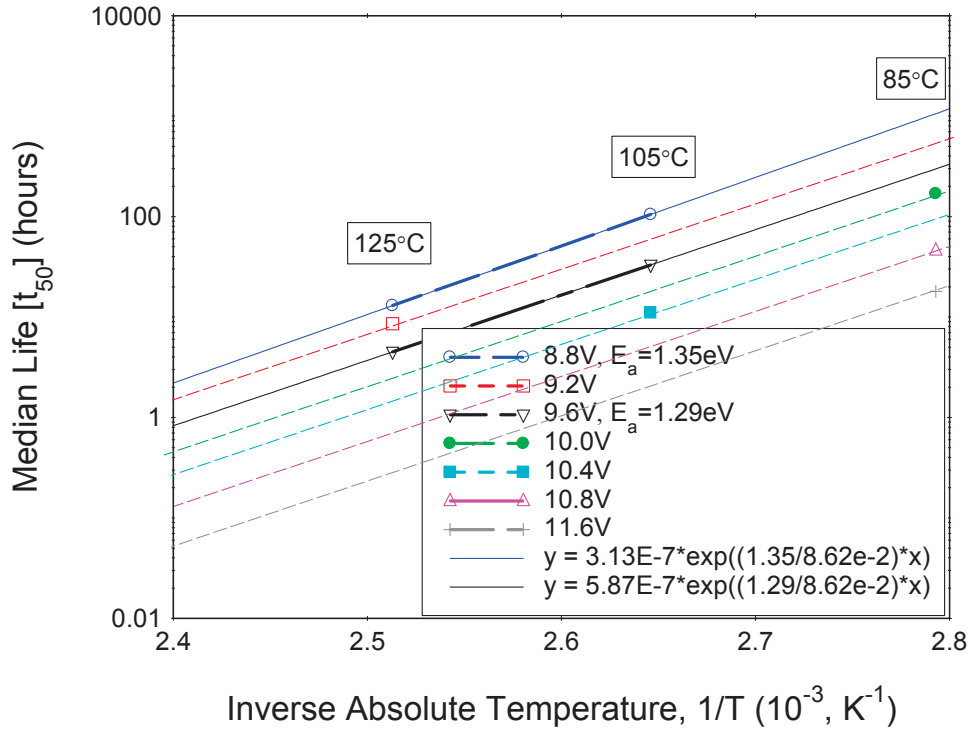


Figure 4-3. Manufacturer A Temperature Acceleration

A temperature acceleration graph for Manufacturer B was not plotted from the test data. The voltage acceleration graph was already severely compromised by the introduction of a new failure mechanism at high test voltages. It is unfortunate that a useful temperature acceleration model cannot be inferred from these data.

5.0 SUMMARY AND CONCLUSIONS

This report presents the accelerated life test data to date for 220 μF , 4 V tantalum polymer capacitors. Testing did not progress as far as expected, but the testing limitations are now better understood, which will allow for further progress next year.

Accelerated life tests are designed to test at high voltages in order to predict behavior at low voltages. It is a delicate balancing act to accelerate conditions enough to produce meaningful wear-out data in a short amount of time without introducing a completely different failure mechanism.

The results of the time-to-failure data of Manufacturer B highlight that caution must be taken when accelerating test conditions. The data obtained for Manufacturer B are not currently useful to establish an acceleration model. Subjecting the devices to such high voltages (12.4 V for a 4 V part) introduced a new failure mechanism, skewing the time-to-failure results.

However, even after the test voltage for the Manufacturer B parts was reduced to 10 V, which produced meaningful results for the Manufacturer A parts, the Manufacturer B parts still demonstrated evidence of anti-wear-out behavior. It is possible that for the Manufacturer B parts, the dominant failure mechanism at application conditions may be de-doping of the polymer with resulting capacitance loss and ESR increase rather than dielectric breakdown. This possibility should be further investigated.

The data collected for Manufacturer A resulted in a very promising acceleration model that predicts very long life at rated voltage and 85°C. With suitable voltage derating, tantalum polymer technology could easily be used in appropriate high-reliability space applications.

6.0 REFERENCES

- [1] Reed, Erik K. *Characterization of Tantalum Polymer Capacitors: NEPP 2005*. Available at: <http://nepp.nasa.gov/docuploads/0EA22600-8AEC-4F47-9FE49BAABEAB569C/Tantalum%20Polymer%20Capacitors%20FY05%20Final%20Report.pdf>
- [2] Reed, Erik K. *Characterization of Tantalum Polymer Capacitors: NEPP 2006*, JPL CL#07-1924, October 9, 2007.
- [3] Paulsen, Jonathan L., Reed, Erik K., and Kelly, Jeffrey N., “Reliability of Tantalum Polymer Capacitors,” *CARTS-Europe 2004*, Nice, France, Oct. 18–21, 2004, pp. 33–39.
- [4] Reed, Erik, Haddox, George, “Reliability of High-Voltage Tantalum Polymer Capacitors,” *CARTS USA 2011*, Jacksonville, Florida, March 28–31, 2011, pp. 195–207.